MAXIMALLY ENERGY-CONCENTRATED DIFFERENTIAL WINDOW FOR PHASE-AWARE SIGNAL PROCESSING USING INSTANTANEOUS FREQUENCY

Tsubasa Kusano, Kohei Yatabe, Yasuhiro Oikawa

Department of Intermedia Art and Science, Waseda University, Tokyo, Japan

ABSTRACT

The short-time Fourier transform (STFT) is widely employed in nonstationary signal analysis, whose property depends on window functions. Instantaneous frequency in STFT, the time-derivative of phase, is recently applied to many applications including spectrogram reassignment. The computation of instantaneous frequency requires STFT with the window and STFT with the (time-)differential window, i.e., the computation of instantaneous frequency depends on both the window function and its time derivative. To obtain the instantaneous frequency accurately, the sidelobe of frequency response of differential window should be reduced because the sidelobe causes mixing of multiple components. In this paper, we propose window functions suitable for computing the instantaneous frequency which are designed based on minimizing the sidelobe energy of the frequency response of the differential window.

Index Terms— Short-time Fourier transform (STFT), instantaneous frequency, differential window, discrete prolate spheroidal sequences (DPSS), spectrogram reassignment.

1. INTRODUCTION

The short-time Fourier transform (STFT) [1] is a time-frequency analysis method, which is widely employed in nonstationary signal analysis and processing owing to its simplicity and well-understood structure [2–20]. The properties of STFT are fully characterized by a window function. Thus, designing a better window according to the property of each application is important for improving the performance of the applications.

Many applications of STFT focus on its spectrogram (the squared magnitude of STFT) since the spectrogram can be easily interpreted as the energy distribution in the time-frequency domain [2, 3]. In contrast, the phase (the complex argument) of STFT had been ignored due to its complicated structure. However, recently, phase-aware techniques are receiving much interest [4–20]. The phase of STFT is not easy to consider directly because the observed phase is wrapped into $[-\pi, \pi)$. Instead, the derivative of phase is considered in some applications such as phase vocoder [4, 5], time-frequency mask estimation [6], spectrogram reassignment [7–11], synchrosqueezing [12–16] and phase conversion [17–19]. The time-derivative of phase is called the instantaneous frequency, and the frequency-derivative of phase is called the group delay [20].

The standard computation method for the instantaneous frequency was proposed by Auger and Flandrin [8], which computes the instantaneous frequency by STFT with the window and STFT with the (time-)differential window (see Sec.2.1). In other words, the computed instantaneous frequency depends on both the window and its differential window. The computed instantaneous frequency is affected by the sidelobes of the frequency response of the differential window. For example, the instantaneous frequency of a signal composed of two sinusoids whose frequencies are sufficiently different is ideally constant in time on each frequency. However, in practice, the computed instantaneous frequency is not constant because the sidelobe causes mixing of multiple components. To estimate the ideal instantaneous frequency, it is necessary to reduce the sidelobe of the frequency response of the differential window.

Many window functions have been proposed aiming to obtain a better STFT from various viewpoints such as frequency responses [21–26], and the numerical stability in signal processing [27–31]. For reducing the sidelobe of the frequency response of the differential window, some windows took into account the continuity at the edges of the windows related to frequency responses of the differential window [25, 26]. However, no method explicitly considers the frequency response of the differential window. If the window function can be designed to reduce sidelobes of the differential window, the STFT having a good property suitable for instantaneous frequency computation should be obtained.

Therefore, in this paper, we propose the window functions which are designed to minimize the sidelobe energy of frequency response of the time-derivative window for the instantaneous frequency computation. In the proposed method, the problem is formulated as the maximization of the frequency-domain energy at the low frequency of the differential window, equivalent to the minimization of sidelobe energy, similar to Slepian's maximally-energy concentration method [22]. Then, its efficient computation method is also proposed. The effectiveness of the proposed method is confirmed by the instantaneous frequency computation and the application to the spectrogram reassignment.

2. PRELIMINARIES

In this preliminary section, a simple derivation of the instantaneous frequency computation formula of STFT [8] and the Slepian window [22] behind the proposed method are explained.

2.1. Computation of instantaneous frequency using STFT

STFT of a discrete signal $\mathbf{x} \in l^2(\mathbb{Z})$ with a continuous window function $g \in L^2(\mathbb{R})$ is defined as [11]

$$(\mathcal{V}_g\mathbf{x})(t, f) = \sum_{n\in\mathbb{Z}} \mathbf{x}[n] g(n - t) \mathrm{e}^{-\mathrm{i}2\pi f n}, \qquad (1)$$

where $\mathbf{x}[n]$ is nth element of $\mathbf{x}$, $t \in \mathbb{R}$, $f \in [-\frac{1}{2}, \frac{1}{2}]$, and $\mathrm{i} = \sqrt{-1}$. The instantaneous frequency, the time derivative of phase $\arg\left((\mathcal{V}_g\mathbf{x})(t, f)\right)$, is given by

$$\frac{\partial}{\partial t}\arg\left((\mathcal{V}_g\mathbf{x})(t, f)\right) = \Im\left\{\frac{1}{\mathcal{V}_g\mathbf{x}} \cdot \frac{\partial}{\partial t}\mathcal{V}_g\mathbf{x}\right\}, \qquad (2)$$

where $\Im\{z\}$ is the imaginary part of z. Here, the time-derivative of STFT can be rewritten as

$$\frac{\partial}{\partial t}(\mathcal{V}_g\mathbf{x})(t,f) = -\sum_{n\in\mathbb{Z}}\mathbf{x}[n]\frac{\mathrm{d}g}{\mathrm{d}t}(n-t)\mathrm{e}^{-\mathrm{i}2\pi fn} = -(\mathcal{V}_{g'}\mathbf{x})(t,f), \tag{3}$$

where $g' = \mathrm{d}g/\mathrm{d}t$ is differential window. Hence, the instantaneous frequency of STFT can be computed by [8]

$$\frac{\partial}{\partial t}\arg\left((\mathcal{V}_g\mathbf{x})(t,f)\right) = -\Im\left\{\frac{(\mathcal{V}_{g'}\mathbf{x})(t,f)}{(\mathcal{V}_g\mathbf{x})(t,f)}\right\}. \tag{4}$$

According to Eq. (4), the instantaneous frequency can be computed by STFT using the window function g and its differential window g'. Hence, the computed instantaneous frequency depends on both window g and its differential window g'.

2.2. Time-limited sequence with most concentrated spectrum

Slepian considered time-limited sequence whose frequency response is maximally concentrated in low-frequency band $[-W,W]$ ($W\in[0,\frac{1}{2})$) [22]. The ratio of the total energy of $\mathbf{g}\in l^2(\mathbb{Z})$ and the banded energy in $[-W,W]$ of $\mathbf{g}$ is represented as

$$\lambda(\mathbf{g}) = \frac{\int_{-W}^{W}|(\mathcal{F}\mathbf{g})(f)|^2 df}{\int_{-\frac{1}{2}}^{\frac{1}{2}}|(\mathcal{F}\mathbf{g})(f)|^2 df}, \tag{5}$$

where

$$(\mathcal{F}\mathbf{g})(f) = \sum_{n\in\mathbb{Z}}\mathbf{g}[n]\mathrm{e}^{-\mathrm{i}2\pi fn}. \tag{6}$$

In the case that $\mathbf{g}$ is time-limited in N samples, i.e.,

$$\mathbf{g}[n] = \begin{cases}\mathbf{v}[n] & (n=0,1,\dots,N-1)\\ 0 & \text{(otherwise)}\end{cases}, \tag{7}$$

Eq. (5) can be rewritten as

$$\lambda(\mathbf{g}) = \lambda(\mathbf{v}) = \frac{\mathbf{v}^{\mathrm{T}}\mathbf{S}_N\mathbf{v}}{\mathbf{v}^{\mathrm{T}}\mathbf{v}}, \tag{8}$$

where $\mathbf{v}\in\mathbb{R}^N$, $\mathbf{v}^{\mathrm{T}}$ is the transpose of $\mathbf{v}$, and $\mathbf{S}_N\in\mathbb{R}^{N\times N}$ is the real-symmetric matrix. The elements of $\mathbf{S}_N$ are given by $\mathbf{S}_N[m,n] = \mathrm{sinc}(2W(m-n))$, where $\mathrm{sinc}(x) = \sin(\pi x)/\pi x$ if $x\neq 0$, and $\mathrm{sinc}(x) = 1$ if $x = 0$. Then, the solution to the problem of maximizing Eq. (5) is obtained by solving the following eigenvalue problem:

$$\mathbf{S}_N\mathbf{v} = \lambda\mathbf{v}. \tag{9}$$

It is known that the eigenvalues of Eq. (9) are nondegenerate and take values between 0 and 1, i.e., $1>\lambda_0>\lambda_1>\cdots>\lambda_{N-1}>0$. In addition, the eigenvectors $\mathbf{v}_k$ corresponding to eigenvalues λ_k have the following properties revealed by Slepian [22]:

$$\textbf{Orthogonality:}\quad \mathbf{v}_j^{\mathrm{T}}\mathbf{v}_k = 0 \quad \text{for } j\neq k, \tag{10}$$

$$\textbf{Symmetry:}\quad \mathbf{v}_k[n] = (-1)^k\mathbf{v}_k[N-n-1], \tag{11}$$

where their norm and signs were determined so that

$$\|\mathbf{v}_k\| = 1, \quad \sum_{n=0}^{N-1}\mathbf{v}_k[n]\geq 0 \quad \text{for } k=0,1,\dots,N-1, \tag{12}$$

and $\|\cdot\|$ is the Euclidian norm. The eigenvector $\mathbf{v}_0$ corresponding to the largest eigenvalue λ_0 is the solution for the problem of maximizing Eq. (5) which is referred to the Slepian window.

$\mathbf{S}_N$ is positive definite, but finding the eigenvalues of $\mathbf{S}_N$ is ill-conditioned for numerical computation because the most eigenvalues of $\mathbf{S}_N$ are concentrated close to 1 or 0. In practice, eigenvectors $\mathbf{v}_k$ are obtained by solving the following eigenvalue problem instead of Eq. (9) [32,33]:

$$\mathbf{T}_N\mathbf{v} = \sigma\mathbf{v}, \tag{13}$$

where $\mathbf{T}_N\in\mathbb{R}^{N\times N}$ is the tridiagonal matrix whose elements are

$$\mathbf{T}_N[m,n] = \begin{cases}\frac{1}{2}m(N-m) & (n=m-1)\\ (\frac{N-1}{2}-m)^2\cos(2\pi W) & (n=m)\\ \frac{1}{2}(m+1)(N-1-m) & (n=m+1)\\ 0 & (|n-m|>1)\end{cases}. \tag{14}$$

$\mathbf{T}_N$ commutes with $\mathbf{S}_N$, i.e., $\mathbf{S}_N\mathbf{T}_N = \mathbf{T}_N\mathbf{S}_N$. Thus, the eigenvectors of $\mathbf{T}_N$ are also the eigenvectors of $\mathbf{S}_N$. Since $\mathbf{T}_N$ is known to have better eigenvalue distribution than $\mathbf{S}_N$, the target eigenvector can be obtained by performing the eigenvalue decomposition to $\mathbf{T}_N$.

3. PROPOSED METHOD

In this section, we propose a window designing method to reduce the influence of the sidelobe of the differential window on the instantaneous frequency computation. The proposed window is designed to minimize the sidelobe energy of the frequency response of the differential window, which causes mixing of multiple components. At first, we formulate the optimal window design as the generalized eigenvalue problem. Then, the efficient computation method of its solution is introduced.

3.1. Maximally energy-concentrated differential window

To achieve the good frequency response of the differential window, the energy concentration problem of the differential window is considered, like the Slepian window. We consider a symmetric window, as many window designs in the literature [21,25,26,30]. Assuming the symmetry of the window function, its derivative is always anti-symmetric. Based on Eq. (8), designing the window function whose derivative is maximally energy-concentrated is formulated as

$$\begin{aligned}&\underset{\mathbf{w}}{\text{maximize}} && \frac{\mathbf{z}^{\mathrm{T}}\mathbf{S}_N\mathbf{z}}{\mathbf{z}^{\mathrm{T}}\mathbf{z}}\\ &\text{subject to} && \mathbf{D}\mathbf{w} = \mathbf{z}\\ &&& \mathbf{z}[n] = -\mathbf{z}[N-n-1]\\ &&& \text{for } n=0,1,\dots,N-1,\end{aligned} \tag{15}$$

where $\mathbf{D}\in\mathbb{R}^{N\times N}$ is a finite-dimensional approximation matrix of the differential operator. To solve this problem, we first solve the subproblem about $\mathbf{z}$ in Eq. (15) and then find $\mathbf{w}$. The first subproblem about $\mathbf{z}$ is written as

$$\underset{\mathbf{z}}{\text{maximize}}\quad \frac{\mathbf{z}^{\mathrm{T}}\mathbf{S}_N\mathbf{z}}{\mathbf{z}^{\mathrm{T}}\mathbf{z}}\quad \text{subject to}\quad \mathbf{A}\mathbf{z} = \mathbf{0}, \tag{16}$$

where $\mathbf{A}\mathbf{z} = \mathbf{0}$ is the linear equation corresponding to the anti-symmetric constraint $\mathbf{z}[n] = -\mathbf{z}[N-n-1]$ in Eq. (15). After solving Eq. (16), the objective window $\mathbf{w}$ can be obtained by solving $\mathbf{D}\mathbf{w} = \mathbf{z}$. In other words, the window function can be obtained by estimating the original window $\mathbf{w}$ from the discretized differential window $\mathbf{z}$ (whose detail is shown in Sec. 3.2).

Eq. (16) can be reformulated as a generalized eigenvalue problem through calculating a basis of the null space of $\mathbf{A}$, but it is numerically ill-conditioned likewise Eq. (9). Fortunately, the solution of Eq. (16) can be efficiently computed from the eigenvector properties of $\mathbf{S}_N$. From Eq. (11), $\mathbf{v}_0$ is symmetric and $\mathbf{v}_1$ is anti-symmetric. In addition, according to Eq. (10) and the inequality $1 > \lambda_0 > \lambda_1 > \cdots > \lambda_{N-1} > 0$, $\mathbf{v}_1$ is the solution of

$$\underset{\mathbf{z}}{\text{maximize}} \;\; \frac{\mathbf{z}^{\mathrm{T}}\mathbf{S}_N\mathbf{z}}{\mathbf{z}^{\mathrm{T}}\mathbf{z}} \quad \text{subject to} \;\; \mathbf{v}_0^{\mathrm{T}}\mathbf{z} = 0. \tag{17}$$

Hence, it is obvious that $\mathbf{v}_1$ is the solution of Eq. (16). That is, as with the conventional Slepian window, the solution of Eq. (16) can be obtained by the eigenvalue decomposition of $\mathbf{T}_N$ in Eq. (14).

3.2. Window estimation from its differential window

In the previous subsection, the estimation method of the maximally energy-concentrated differential window function $\mathbf{z} = \mathbf{v}_1$ is proposed. However, the estimation problem of the window from the differential window remained. In this section, the estimation method of the window from the differential window is introduced.

As calculating the window from the optimized differential window $\mathbf{v}_1$, the spectral integral [11]

$$\mathbf{w} = \mathbf{F}_{M,M}^{*}\mathbf{B}(c)\mathbf{F}_{M,N}\mathbf{v}_1, \tag{18}$$

is considered, where $\mathbf{F}_{M,N} \in \mathbb{C}^{M\times N}$ is the zero-padded discrete Fourier transfrom (DFT) with the DFT length M,

$$\mathbf{F}_{M,N}[m,n] = \frac{1}{\sqrt{M}}\mathrm{e}^{-\mathrm{i}\frac{2\pi mn}{M}}, \tag{19}$$

$\mathbf{F}_{M,M}^{*}$ is the conjugate transpose of $\mathbf{F}_{M,M}$, $\mathbf{B}_M(c) \in \mathbb{C}^{M\times M}$ is the diagonal matrix whose diagonal elements are

$$\mathbf{B}(c)[n,n] = \begin{cases} c & n = 0 \\ M/\mathrm{i}2\pi n & 0 < n \le \lfloor M/2 \rfloor \\ M/\mathrm{i}2\pi(M-n) & \lfloor M/2 \rfloor < n \le M-1 \end{cases}, \tag{20}$$

$\lfloor\cdot\rfloor$ is the floor function, and c is an integral constant which cannot be determined from only the differential window. Hence, c has to be determined from some point of view in the integrated window.

Denoting $\mathbf{w}_0 = \mathbf{F}_{M,M}^{*}\mathbf{B}(0)\mathbf{F}_{M,N}\mathbf{v}_1$, $\mathbf{w}$ is written as $\mathbf{w} = \mathbf{w}_0 + c\mathbf{1}_M$, where $\mathbf{1}_M \in \mathbb{R}^M$ is a vector whose elements are all one. We propose determining c in terms of the maximization of the mainlobe energy as the Slepian window in Sec. 2.2,

$$\underset{c>0}{\text{maximize}} \;\; \lambda(\mathbf{w}_0 + c\mathbf{1}_M). \tag{21}$$

$\lambda(\mathbf{w}_0 + c\mathbf{1}_M)$ is specifically rewritten using Eq. (8) as

$$\lambda(\mathbf{w}_0 + c\mathbf{1}_M) = \frac{\mathbf{w}_0^{\mathrm{T}}\mathbf{S}_M\mathbf{w}_0 + 2\mathbf{1}_M^{\mathrm{T}}\mathbf{S}_M\mathbf{w}_0 c + \mathbf{1}_M^{\mathrm{T}}\mathbf{S}_M\mathbf{1}_M c^2}{\mathbf{w}_0^{\mathrm{T}}\mathbf{w}_0 + 2\mathbf{1}_M^{\mathrm{T}}\mathbf{w}_0 c + \mathbf{1}_M^{\mathrm{T}}\mathbf{1}_M c^2}.$$

As $\mathbf{1}_M^{\mathrm{T}}\mathbf{1}_M = M$ and $\mathbf{1}_M^{\mathrm{T}}\mathbf{w}_0 = 0$ from the unitarity of $\mathbf{F}_{M,M}^{*}$,

$$\lambda(\mathbf{w}_0 + c\mathbf{1}_M) = \frac{\mathbf{w}_0^{\mathrm{T}}\mathbf{S}_M\mathbf{w}_0 + 2\mathbf{1}_M^{\mathrm{T}}\mathbf{S}_M\mathbf{w}_0 c + \mathbf{1}_M^{\mathrm{T}}\mathbf{S}_M\mathbf{1}_M c^2}{\|\mathbf{w}_0\|^2 + Mc^2}.$$

The necessary condition of $\lambda(c)$ being maxima is

$$\begin{aligned}\frac{\partial\lambda}{\partial c} =& \frac{(2\mathbf{1}_M^{\mathrm{T}}\mathbf{S}_M\mathbf{w}_0 + 2\mathbf{1}_M^{\mathrm{T}}\mathbf{S}_M\mathbf{1}_M c)}{(Mc^2 + \|\mathbf{w}_0\|^2)} \\ &- \frac{2Mc(\mathbf{w}_0^{\mathrm{T}}\mathbf{S}_M\mathbf{w}_0 + 2\mathbf{1}_M^{\mathrm{T}}\mathbf{S}_M\mathbf{w}_0 c + \mathbf{1}_M^{\mathrm{T}}\mathbf{S}_M\mathbf{1}_M c^2)}{(Mc^2 + \|\mathbf{w}_0\|^2)^2} = 0.\end{aligned} \tag{22}$$

Since the denominator of Eq. (22), $Mc^2 + \|\mathbf{w}_0\|^2 > 0$, Eq. (22) can be rewritten as the equation for c,

$$M\mathbf{1}_M^{\mathrm{T}}\mathbf{S}_M\mathbf{w}_0 c^2 + ac - \mathbf{1}_M^{\mathrm{T}}\mathbf{S}_M\mathbf{w}_0\|\mathbf{w}_0\|^2 = 0, \tag{23}$$

where $a = (M\mathbf{w}_0^{\mathrm{T}}\mathbf{S}_M\mathbf{w}_0 - \mathbf{1}_M^{\mathrm{T}}\mathbf{S}_M\mathbf{1}_M\|\mathbf{w}_0\|^2)$. Its solutions are

$$c_{\pm} = \frac{-a \pm \sqrt{d}}{2M\mathbf{1}_M^{\mathrm{T}}\mathbf{S}_M\mathbf{w}_0}, \tag{24}$$

where $d = a^2 + 4M(\mathbf{1}_M^{\mathrm{T}}\mathbf{S}_M\mathbf{w}_0)^2\|\mathbf{w}_0\|^2$. The two solutions in Eq. (24) are real because $d > 0$. Eventually, from

$$-a - \sqrt{d} < 0 < -a + \sqrt{d}, \tag{25}$$

$\mathbf{1}_M^{\mathrm{T}}\mathbf{S}_M\mathbf{w}_0 > 0$, and the constraint $c > 0$, c is calculated as

$$c = \frac{-a + \sqrt{d}}{2M\mathbf{1}_M^{\mathrm{T}}\mathbf{S}_M\mathbf{w}_0}. \tag{26}$$

3.3. Summary of the proposed method

In summary, the proposed window $\mathbf{w}$ and its derivative $\mathbf{v}_1$ are obtained as follows:

Step 1. Apply the eigenvalue decomposition to $\mathbf{T}_N$ and get the eigenvector $\mathbf{v}_1$ corresponding to the second largest eigenvalue.
Step 2. Compute $\mathbf{w}_0 = \mathbf{F}_{M,M}^{*}\mathbf{B}(0)\mathbf{F}_{M,N}\mathbf{v}_1$.
Step 3. Compute c using Eq. (26).
Step 4. Compute $\mathbf{w} = \mathbf{w}_0 + c\mathbf{1}_M$.
Step 5. (optional) Truncate $\mathbf{w}$ to be length N.
Step 6. Output the window $\mathbf{w}$ and its derivative $\mathbf{v}_1$.

Step 5 is an optional step to return the window length from M to N. It will be presented in the next experimental section that the differential window of the truncated proposed window also has a good frequency response.

4. EXPERIMENTS

In this section, the proposed window was compared to the Slepian windows. First, we compared the frequency responses of the window functions, then the error of instantaneous frequency computation using the windows was evaluated. Finally, the windows are applied to the spectrogram reassignment.

4.1. Frequency responses of proposed windows

At first, the shapes and frequency responses of the proposed window and their differential window were compared to those of the Slepian window with two different bandwidths W. In the experiments, the derivative of the Slepian windows are calculated as [11]

$$\mathbf{D}\mathbf{w} = \mathbf{F}_{M,N}^{*}\mathbf{G}_M\mathbf{F}_{M,N}\mathbf{w}, \tag{27}$$

where $\mathbf{G}_M \in \mathbb{C}^{M\times M}$ is the diagonal matrix whose diagonal elements are

$$\mathbf{G}_M[n,n] = \begin{cases} \mathrm{i}2\pi n/M & 0 \le n \le \lfloor M/2 \rfloor \\ \mathrm{i}2\pi(M-n)/M & \lfloor M/2 \rfloor < n \le M-1 \end{cases}. \tag{28}$$

The length of windows and DFT were set to $N = 2^7$ and $M = 2^{12}$.

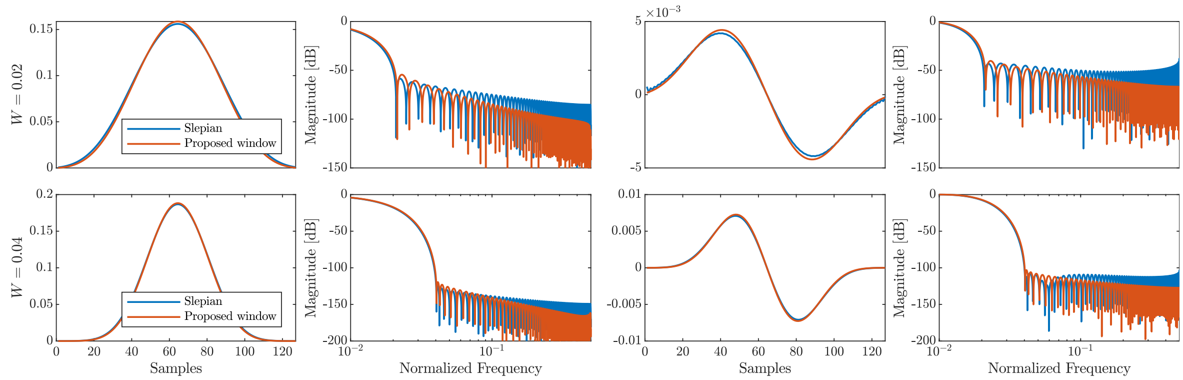

Fig. 1. Results of designed windows. Each column shows (from left to right) the window functions, their frequency responses, their differential windows, and the frequency responses of the differential windows.

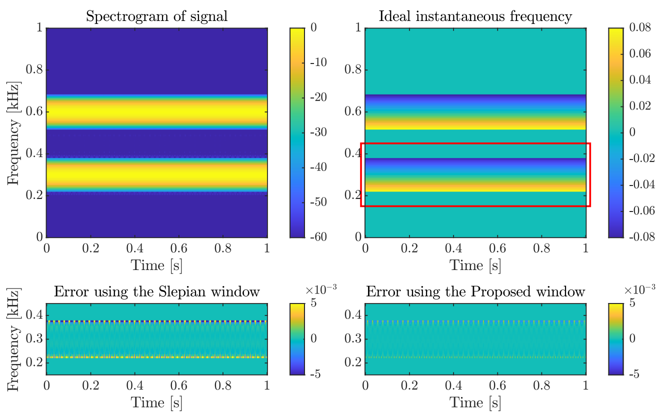

Fig. 2. Instantaneous frequency computed by two different windows. The top row shows the spectrogram of a signal composed of two sinusoids and its ideal instantaneous frequency. The bottom row shows the errors of the computed instantaneous frequency using the Slepian window and that using the proposed window.

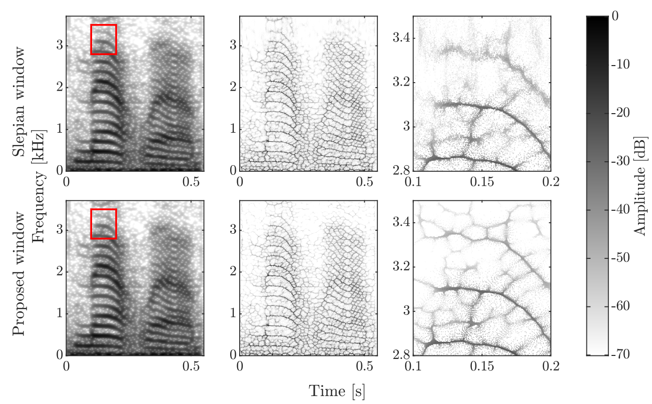

Fig. 3. Spectrogram reassignment with two different windows. Each column shows (from left to right) the spectrograms, the reassigned spectrograms, the enlargement of the reassigned spectrograms in the red box. The top and bottom rows show the results for the Slepian window and the proposed window, respectively.

The proposed windows and the Slepian windows in the cases of bandwidth $W = 0.02, 0.04$ are illustrated in Fig. 1. Their frequency responses were normalized so that the maxima are 0 dB. In both cases of $W = 0.02, 0.04$, the proposed window has better sidelobe decays than the Slepian windows although the highest sidelobe level is slightly higher. Furthermore, the differential windows of the Slepian windows lose sidelobe decays, while the proposed windows retain sidelobe decays.

4.2. Evaluation of instantaneous frequency computation

The proposed window was compared with the Slepian window in terms of the instantaneous frequency computation. The instantaneous frequency of a signal composed of two sinusoids, whose spectrogram is illustrated in Fig. 2, was computed by using two windows shown in the top row of Fig. 1. The results of instantaneous frequency computation are summarized in Fig. 2. Note that the ideal instantaneous frequency represents the instantaneous frequency without the effect of sidelobes. It can be seen that the result of the proposed window has less error than that of the Slepian window. These results suggest that the proposed window reduces the effect of sidelobes on the instantaneous frequency computation owing to the good sidelobe decay of its differential window.

4.3. Application to spectrogram reassignment

The proposed window was applied to the spectrogram reassignment of a speech signal, whose sampling frequency was 7418 Hz. The spectrogram reassignment aims to assign the energy spread by the window function to the correct position using the instantaneous frequency and group delay [10]. The Slepian window and the proposed window, with the length $N = 2^8$ and the bandwidth $W = 0.01$, were used in this experiment. The results are summarized in Fig. 3.

Comparing two reassigned spectrograms in Fig. 3, the reassigned spectrogram using the proposed window is sharper than that of the Slepian window. These results indicate that the proposed window improves the performance of the spectrogram reassignment.

5. CONCLUSION

In this paper, the window function whose differential window is maximally energy-concentrated and its efficient computation are proposed. The proposed window has a good frequency response in terms of the instantaneous frequency estimation. Future work includes the generalization of the proposed method to higher-order derivatives [14–16] and an investigation of its efficient computation.

6. REFERENCES

[1] K. Gröchenig, *Foundations of Time-Frequency Analysis*, Applied and Numerical Harmonic Analysis. Birkhäuser Boston, Boston, MA, 2001.

[2] Y. Ephraim and D. Malah, "Speech enhancement using a minimum-mean square error short-time spectral amplitude estimator," *IEEE Trans. Acoust., Speech, Signal Process.*, vol. 32, no. 6, pp. 1109–1121, Dec. 1984.

[3] T. Virtanen, "Monaural sound source separation by nonnegative matrix factorization with temporal continuity and sparseness criteria," *IEEE Trans. Audio, Speech, Lang. Process.*, vol. 15, no. 3, pp. 1066–1074, Mar. 2007.

[4] J. L. Flanagan and R. M. Golden, "Phase vocoder," *Bell Syst. Tech. J.*, vol. 45, no. 9, pp. 1493–1509, Nov. 1966.

[5] M. Dolson, "The phase vocoder: A tutorial," *Comput. Music J.*, vol. 10, no. 4, pp. 14–27, 1986.

[6] A. Hiruma, K. Yatabe, and Y. Oikawa, "Separating stereo audio mixture having no phase difference by convex clustering and disjointness map," in *Proc. Int. Workshop Acoust. Signal Enhance. (IWAENC)*, Sept. 2018, pp. 266–270.

[7] K. Kodera, C. De Villedary, and R. Gendrin, "A new method for the numerical analysis of non-stationary signals," *Phys. Earth Planet. Inter.*, vol. 12, no. 2–3, pp. 142–150, Aug. 1976.

[8] F. Auger and P. Flandrin, "Improving the readability of time-frequency and time-scale representations by the reassignment method," *IEEE Trans. Signal Process.*, vol. 43, no. 5, pp. 1068–1089, May 1995.

[9] S. A. Fulop and K. Fitz, "Algorithms for computing the time-corrected instantaneous frequency (reassigned) spectrogram, with applications," *J. Acoust. Soc. Am.*, vol. 119, no. 1, pp. 360–371, Jan. 2006.

[10] F. Auger, P. Flandrin, Y.-T. Lin, S. McLaughlin, S. Meignen, T. Oberlin, and H.-T. Wu, "Time-frequency reassignment and synchrosqueezing: An overview," *IEEE Signal Process. Mag.*, vol. 30, no. 6, pp. 32–41, Nov. 2013.

[11] S. Fenet, R. Badeau, and G. Richard, "Reassigned timefrequency representations of discrete time signals and application to the constant-Q transform," *Signal Process.*, vol. 132, pp. 170–176, Mar. 2017.

[12] I. Daubechies, J. Lu, and H. T. Wu, "Synchrosqueezed wavelet transforms: An empirical mode decomposition-like tool," *Appl. Comput. Harmon. Anal.*, vol. 30, no. 2, pp. 243–261, 2011.

[13] S. Meignen, T. Oberlin, and S. McLaughlin, "A new algorithm for multicomponent signals analysis based on synchrosqueezing: With an application to signal sampling and denoising," *IEEE Trans. Signal Process.*, vol. 60, no. 11, pp. 5787–5798, Nov. 2012.

[14] T. Oberlin, S. Meignen, and V. Perrier, "Second-order synchrosqueezing transform or invertible reassignment? Towards ideal time-frequency representations," *IEEE Trans. Signal Process.*, vol. 63, no. 5, pp. 1335–1344, Mar. 2015.

[15] D.-H. Pham and S. Meignen, "High-order synchrosqueezing transform for multicomponent signals analysis—With an application to gravitational-wave signal," *IEEE Trans. Signal Process.*, vol. 65, no. 12, pp. 3168–3178, June 2017.

[16] R. Behera, S. Meignen, and T. Oberlin, "Theoretical analysis of the second-order synchrosqueezing transform," *Appl. Comput. Harmon. Anal.*, vol. 45, no. 2, pp. 379–404, Sept. 2018.

[17] K. Yatabe and Y. Oikawa, "Phase corrected total variation for audio signals," in *Proc. IEEE Int. Conf. Acoust., Speech, Signal Process. (ICASSP)*, Apr. 2018, pp. 656–660.

[18] Y. Masuyama, K. Yatabe, and Y. Oikawa, "Low-rankness of complex-valued spectrogram and its application to phase-aware audio processing," in *Proc. IEEE Int. Conf. Acoust., Speech, Signal Process. (ICASSP)*, May 2019, pp. 855–859.

[19] K. Yatabe, Y. Masuyama, T. Kusano, and Y. Oikawa, "Representation of complex spectrogram via phase conversion," *Acoust. Sci. Technol.*, vol. 40, no. 3, pp. 170–177, 2019.

[20] P. Balazs, D. Bayer, F. Jaillet, and P. L. Søndergaard, "The pole behavior of the phase derivative of the short-time Fourier transform," *Appl. Comput. Harmon. Anal.*, vol. 40, no. 3, pp. 610–621, May 2016.

[21] C. L. Dolph, "A current distribution for broadside arrays which optimizes the relationship between beam width and side-lobe level," *Proc. IRE*, vol. 34, no. 6, pp. 335–348, June 1946.

[22] D. Slepian, "Prolate spheroidal wave functions, Fourier analysis, and uncertainty-V: The discrete case," *Bell Syst. Tech. J.*, vol. 57, no. 5, pp. 1371–1430, May 1978.

[23] F. J. Harris, "On the use of windows for harmonic analysis with the discrete Fourier transform," *Proc. IEEE*, vol. 66, no. 1, pp. 51–83, 1978.

[24] J. Kaiser and R. Schafer, "On the use of the I_0-sinh window for spectrum analysis," *IEEE Trans. Acoust., Speech, Signal Process.*, vol. 28, no. 1, pp. 105–107, Feb. 1980.

[25] A. Nuttall, "Some windows with very good sidelobe behavior," *IEEE Trans. Acoust., Speech, Signal Process.*, vol. 29, no. 1, pp. 84–91, Feb. 1981.

[26] H. Kawahara, K. Sakakibara, M. Morise, H. Banno, T. Toda, and T. Irino, "A new cosine series antialiasing function and its application to aliasing-free glottal source models for speech and singing synthesis," in *Proc. Annu. Conf. Int. Speech. Commun. Assoc. (Interspeech)*, Aug. 2017, pp. 1358–1362.

[27] Z. Cvetkovic, "On discrete short-time Fourier analysis," *IEEE Trans. Signal Process.*, vol. 48, no. 9, pp. 2628–2640, 2000.

[28] M. R. Wilbur, T. N. Davidson, and J. P. Reilly, "Efficient design of oversampled NPR GDFT filterbanks," *IEEE Trans. Signal Process.*, vol. 52, no. 7, pp. 1947–1962, 2004.

[29] J. Jiang, S. Ouyang, and F. Zhou, "Design of NPR DFT-modulated filter banks via iterative updating algorithm," *Circuits, Syst., Signal Process.*, vol. 32, no. 3, pp. 1351–1362, 2013.

[30] N. Perraudin, N. Holighaus, P. L. Søndergaard, and P. Balazs, "Designing Gabor windows using convex optimization," *Appl. Math. Comput.*, vol. 330, pp. 266–287, Aug. 2018.

[31] T. Kusano, Y. Masuyama, K. Yatabe, and Y. Oikawa, "Designing nearly tight window for improving time-frequency masking," in *Proc. Int. Congr. Acoust. (ICA)*, 2019, pp. 2885–2892.

[32] D. M. Gruenbacher and D. R. Hummels, "A simple algorithm for generating discrete prolate spheroidal sequences," *IEEE Trans. Signal Process.*, vol. 42, no. 11, pp. 3276–3278, 1994.

[33] T. Verma, S. Bilbao, and T. H. Y. Meng, "The digital prolate spheroidal window," in *Proc. IEEE Int. Conf. Acoust., Speech, Signal Process. (ICASSP)*, 1996, vol. 3, pp. 1351–1354.